Proceedings of the ASME 2021 Heat Transfer Summer Conference
HT2021
June 16-18, 2021, Virtual, Online

HT2021-63004

# INVESTIGATION OF BUOYANCY EFFECTS IN ASYMMETRICALLY HEATED NEAR-CRITICAL FLOWS OF CARBON DIOXIDE IN HORIZONTAL MICROCHANNELS USING INFRARED THERMOGRAPHY

Lindsey V. Randle Brian M. Fronk\*

School of Mechanical, Industrial, and Manufacturing Engineering
Oregon State University
Corvallis, Oregon, 97331
Email: brian.fronk@oregonstate.edu

#### **ABSTRACT**

In this study, we use infrared thermography to calculate local heat transfer coefficients of top and bottom heated flows of near-critical carbon dioxide in an array of parallel microchannels. These data are used to evaluate the relative importance of buoyancy for different flow arrangements. A Joule heated thin wall made of Inconel 718 applies a uniform heat flux either above or below the horizontal flow. A Torlon PAI test section consists of three parallel microchannels with a hydraulic diameter of 923  $\mu m$ . The reduced inlet temperature ( $T_R = 1.006$ ) and reduced pressure  $(P_R = 1.03)$  are held constant. For each heater orientation, the mass flux (520 kgm<sup>-2</sup>s<sup>-2</sup>  $\leq G \leq 800 \text{ kgm}^{-2}\text{s}^{-2}$ ) and heat flux (4.7 W cm<sup>-2</sup>  $\leq q$ "  $\leq 11.1 \text{ W cm}^{-2}$ ) are varied. A 2D resistance network analysis method calculates the bulk temperatures and heat transfer coefficients. In this analysis, we divide the test section into approximately 250 segments along the streamwise direction. We then calculate the bulk temperatures using the enthalpy from the upstream segment, the heat flux in a segment, and the pressure. To isolate the effect of buoyancy, we screen the data to omit conditions where flow acceleration may be important or where relaminarization may occur. In the developed region of the channel, there was a 10 to 15 percent reduction of the local heat transfer coefficients for the upward heating mode compared to downward heating with the same mass and heat fluxes. Thus buoyancy effects should be considered when developing correlations for these types of flow.

\*Address all correspondence to this author.

 $\label{thm:convective} \textit{Keywords: supercritical ; infrared thermography, convective heat transfer}$ 

#### **NOMENCLATURE**

 $c_p$  Specific heat capacity

G Mass Flux

h Specific enthalpy

IR infrared

*in* Mass flow rate

Per Perimeter

q" Heat flux

sCO<sub>2</sub> Supercritical carbon dioxide

 $\alpha$  Convective heat transfer coefficient

 $\beta$  Coefficient of thermal expansion

#### INTRODUCTION AND PRIOR WORK

Supercritical carbon dioxide is a promising working fluid for the cooling of high flux electronics [1]. Near the critical point, carbon dioxide exhibits a sharp increase in convective heat transfer coefficients due to an spike in specific heat capacity and Prandtl number. In this region, many other properties also change drastically, including density. This can lead to axial flow acceleration (which tends to degrade heat transfer) and buoyancy effects which can either enhance or degrade the turbulent transport.

There has been significant investigation of heating of supercritical carbon dioxide in uniformly heated, circular tubes [2]. This has led to many empirical and semi-empirical relations to predict heat transfer near the critical point [3]. There has been very limited study of near-critical heat transfer in non-uniformly heated channels.

Jajja et al. [4,5] conducted a series of near-critical heat transfer studies in non-uniformly heated microchannel and micro-pin arrays. They conducted experiments at heat fluxes from 5 to 50 W cm<sup>-2</sup>. They found that existing supercritical correlations predicted heat transfer relatively poorly. However, they could not isolate the effects of top or bottom heating versus uniform heating due to conjugate heat transfer (mostly fin effects, axial conduction and heat spreading) within the test section. More recently, Jajja [6] developed an approach to measure local supercritical heat transfer near the critical point using an infrared thermography technique. He was able to isolate the heated surface to a single wall by machining an microchannel array in an electrically and thermally insulating material, sealed with a thin joule heated Inconel-718 wall on one side. He conducted experiments in microchannels with hydraulic diameter of 923 µm and an aspect ratio of 3.33. Experiments were conducted with horizontal flow; and with an upward, relative to gravity, heating mode for heat fluxes from 5 to 11 W cm<sup>-2</sup>; and with reduced temperatures from 0.99 to 1.002. He confirmed that existing supercritical heat transfer correlations [7–9] developed for uniformly heated tubes did not predict data well for non-uniformly heated channels, with significant under predictions.

Jajja [6] screened his data for the influence of flow acceleration and buoyancy using the criteria of McEligot et al. [10] and Petukhov and Polyakov [11], respectively. Flow acceleration was not expected to be important for his data. However, the criteria of Petukhov and Polyakov suggested that buoyancy would influence heat transfer for nearly all his data. Since experiments were only conducted in a single orientation, and there was no direct observation of the distortion of the temperature or velocity fields, the effects could not be quantified. Thus, the objective of this work is to conduct single heated wall experiments using the same test facility as Jajja in downwards, relative to gravity, heating mode.

## METHODS AND MATERIALS Test Loop

We conducted experiments in an approximately single pressure flow loop, as shown in Figure 1. A detailed description of the is available in Jajja et al. [4], but summarized here for completeness. The test loop is a closed system with the main components of an electric pre-heater, a post-cooler, a gear pump, and a piston accumulator. The tube-in-tube pre-heater is powered by two 1.5 kW cartridge heaters in the inner tube. It is used to heat the carbon dioxide in the annulus to the desired inlet temperature before it enters the test section. The tube-in-tube post-cooler is

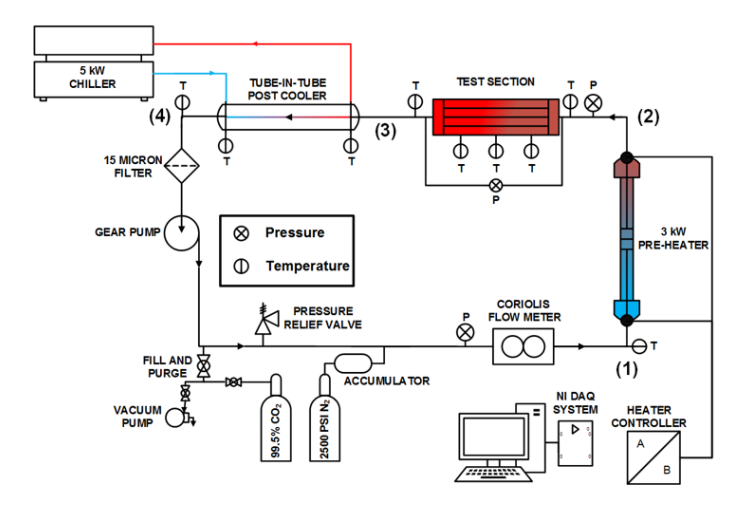


FIGURE 1. Schematic of the experimental facility

directly after the test section and is cooled with a 5 kW chiller. This component reduces the temperature of the carbon dioxide to near room temperature, where it can be pumped using a magnetically coupled, variable speed micro-pump gear pump (Micropump Model GC M23). A 0.95 L piston accumulator controls the loop pressure using high-pressure nitrogen controlled by a high-pressure regulator. The loop is initially charged with liquid carbon dioxide, which is then pressurized to supercritical pressures by the adjusting the accumulator pressure.

Calibrated T type thermocouples measure the temperature throughout the loop with an uncertainty of  $\pm~0.5^{\circ}\text{C}$ . Including at the inlet and outlet of the test section; see Figure 1 for all thermocouple locations. A Rosemount 3051SMV pressure transducer measures both the differential pressure in the range of 0 to 62.2 kPa across the test section and the absolute pressure in the range of 0 to 24.8 MPa in the test section. A Coriolis flowmeter measures the carbon dioxide mass flow rate with a nominal uncertainty of 0.1% and is used to inform adjustments to the pump to achieve the desired flow rate.

#### **Test Section**

The test section consists of three parallel microchannels made from Torlon 4203. Torlon is an electrically and thermally insulating plastic material. The channels are 2 mm in width, 50 mm in length, and 600  $\mu$ m in height. Figure 2 shows an exploded diagram of the test section. The carbon dioxide enters the header section perpendicular to the channels. The fluid then continues through the channels to another header section at the exit, which is also perpendicular to the channels. The wall opposite the inlet and outlet is the Joule heated wall. The heated wall is made of Inconel 718 and spans all three of the channels and the header regions. A direct electric current is applied across the heated

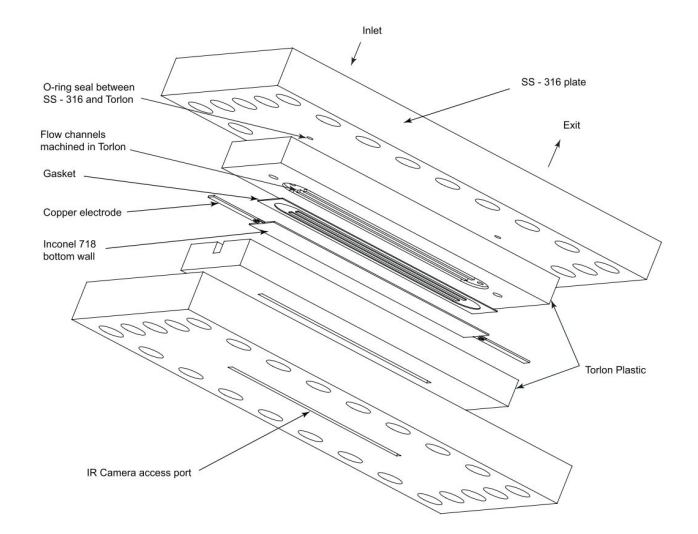


**FIGURE 2**. Exploded view of the infrared test section from [6]

wall using a TDK Lambda power supply. A small viewing window allows a FLIR A325sc inferred camera to directly view the outside of the Inconel over the center channel. The camera is calibrated with a calibrated blackbody as described in Jajja [6]. The outside of the Inconel is coated with Pyromark 1200, which has a known emissivity of 0.95 and is durable in high heat environments. This allows the infrared camera to record accurate surface temperatures of the Inconel, which are then used to evaluate the local heat transfer coefficients of the carbon dioxide, as described below.

#### **Data Analysis**

The IR camera provides a 2D array of Inconel heater surface temperatures. These temperatures are assumed to be uniform through the heater thickness, as the Inconel is thin enough that conduction parallel to the face is negligible ( $Bi_{spanwise} = 0.01563$ and  $Bi_{flowdirection} = 0.000025$  [6]). We assume that the flow is distributed equally among the 3 channels. The bulk carbon dioxide temperatures are found by dividing the channel into a series of nodes in the flow direction. Each node is the length of one pixel from the IR camera (approximately 0.2 mm), and there are about 250 nodes in the channel. Each node's bulk temperature is found using the enthalpy from the previous node and the energy from the heated wall in that area. The channel inlet temperature is used to find the enthalpy of the first node; this temperature is found using the measured temperature right before the header section and the heat from the header section. The total power into the heater is measured, and the heat flux is assumed to be uniform, as the resistivity change of Inconel-718 in the temperature range of interest is negligible. We assume the the heat generated in the section of the Inconel touching the separating walls is distributed through the channels. The bulk temperatures together with the measured wall temperatures are then used to calculate the local heat transfer coefficients. This calculation also accounts for the heat loss by radiation from the exposed heated sidewall. The uncertainties for the heat transfer coefficients were found using the sequential perturbation method described by Figliola and Beasley [12]. This method was chosen due to the large number of surface temperature measurements (>2500).

#### **RESULTS**

We conducted experiments in a horizontal orientation, at two different heat fluxes, two mass fluxes, and with upward and downward heating modes. The nominal reduced inlet temperature ( $T_R = 1.006$ , T = 32.8 °C) and nominal reduced pressure ( $P_R = 1.03$ , P = 7740 kPa) are held constant. We selected operating conditions for which buoyancy was expected to be important, as predicted by the Petukhov and Polyakov [11] screening criteria.

### Screening of Data for Flow Acceleration and Buoyancy Effects

Ideally, we would like to compare only buoyancy effects between the top and bottom heated conditions. In addition to buoyancy, flow acceleration can significantly alter thermal transport. Bulk acceleration in the flow can suppress turbulent thermal transport by reducing near-wall fluid motion towards the center of the channel. If this suppression is significant enough, it can go so far as to cause the flow to relaminarize. Therefore we screen for relaminarization by evaluating the acceleration parameter from McEligot et al. [10] (equation 1), as recommended by Jackson and McEligot [13].

$$K_{v} = 4\left(\frac{Per_{heat}}{Per_{wet}}\right)q^{+} \tag{1}$$

$$q^{+} = \frac{\beta q"_{wall}}{G_{chan}c_{p}} \tag{2}$$

The acceleration effects on the flow are considered negligible if  $K_{\nu}$  is less than 3e-6. All of the cases considered in this paper are below this threshold. The highest average  $K_{\nu}$  value of 2.95e-8 was from the bottom heated case (q" = 11.11 W cm<sup>-2</sup>, G = 533 kg m<sup>-2</sup>). Therefore it is reasonable to assume that the acceleration effects in this study are negligible.

The data were then screened for the potential effects of buoyancy in horizontal ducts using the criteria of Petukhov and Polyakov [11]. They defined a threshold criterion based on a heat flux Grashof number. When the ratio is greater than one, buoyancy effects are predicted to be significant enough to impact the turbulent thermal transport. As shown in Figure 3, buoyancy is expected to be relevant for all of the data in this study.

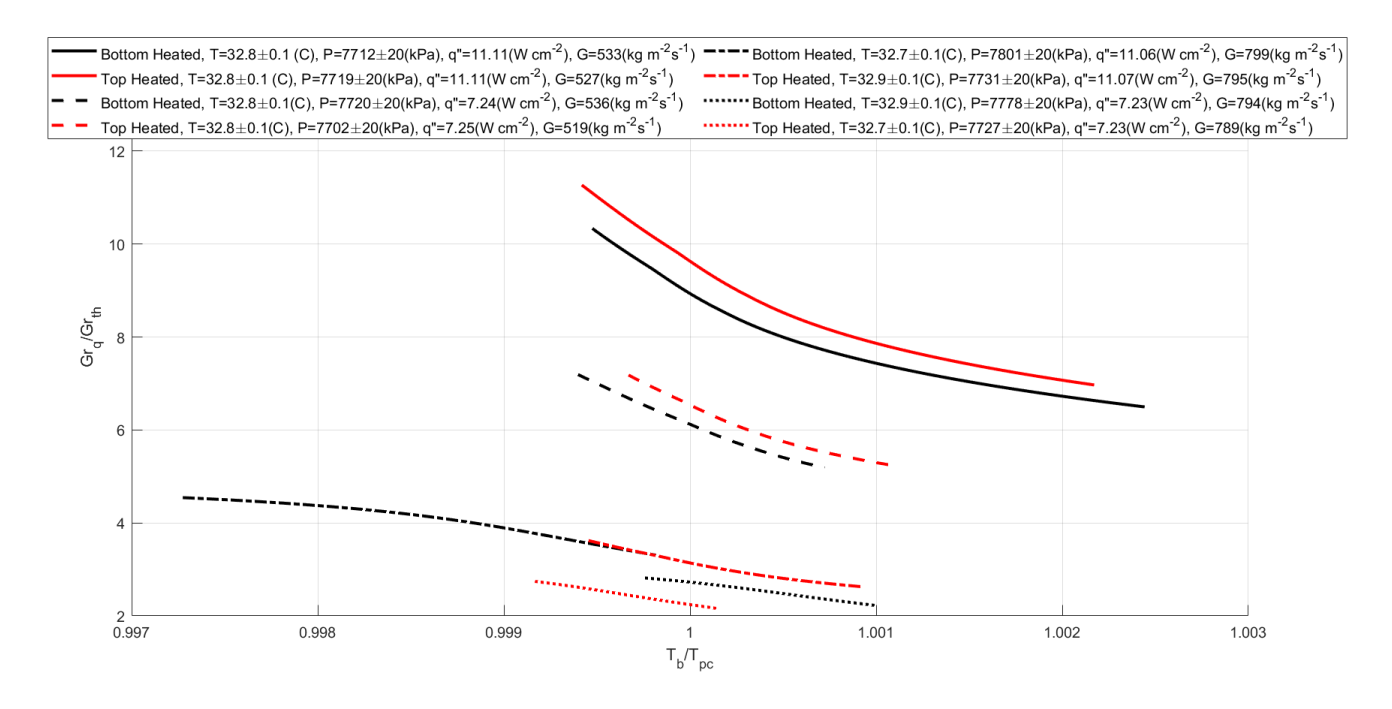
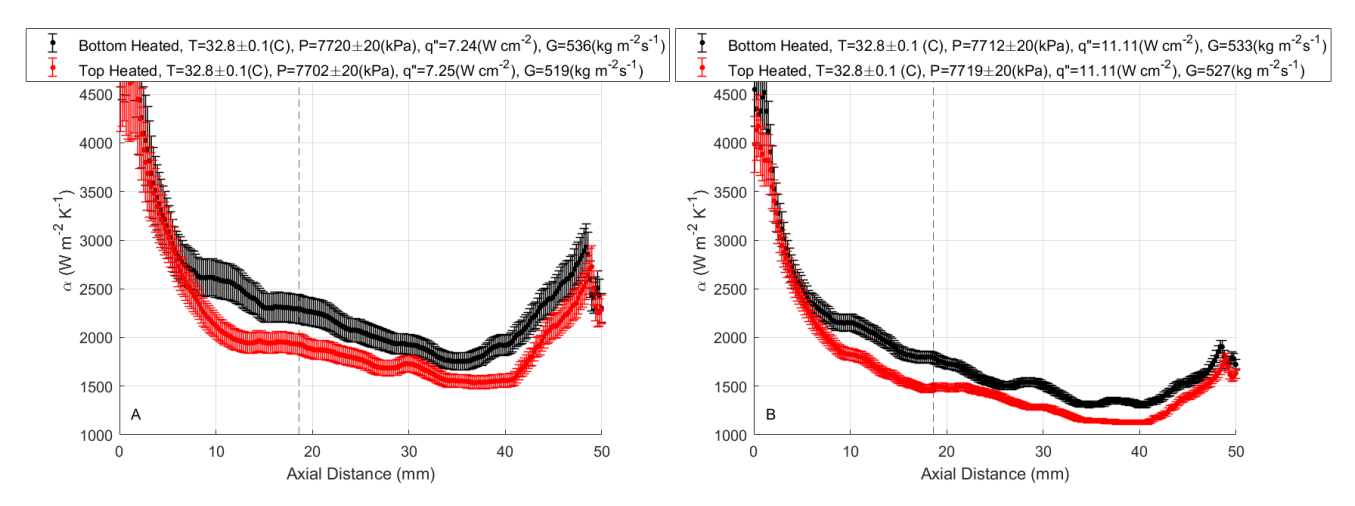


FIGURE 3. Buoyancy Criteria of Petukhov and Polyakov [11]



**FIGURE 4**. Asymmetrically Bottom and Top Heated Conditions with Constant Mass Flux ( $G = 520 \text{ kg m}^{-2} \text{ s}^{-1}$ ). A)  $q'' = 7.25 \text{ W cm}^{-2}$ , B)  $q'' = 11.1 \text{ W cm}^{-2}$ 

#### **Effect of Heat Flux**

Experiments were performed where the heat flux was varied between  $q^{\prime\prime}=7.23~W~cm^{-2}$  and  $q^{\prime\prime}=11.07~W~cm^{-2}$  and the mass flux was held constant at a nominal  $G=520~kg~m^{-2}~s^{-1}$ . The experiments were run with the test section in both top and bottom heating, with the results shown in Figure 4. The hydrodynamic developing length was estimated according to the

following equation 3 [14]:

$$x_{dev,h} = 3.8Re^{\frac{1}{6}}D_h \tag{3}$$

Figure 4 shows that near the entrance of the channel in the developing region (transition is indicated with a dashed vertical

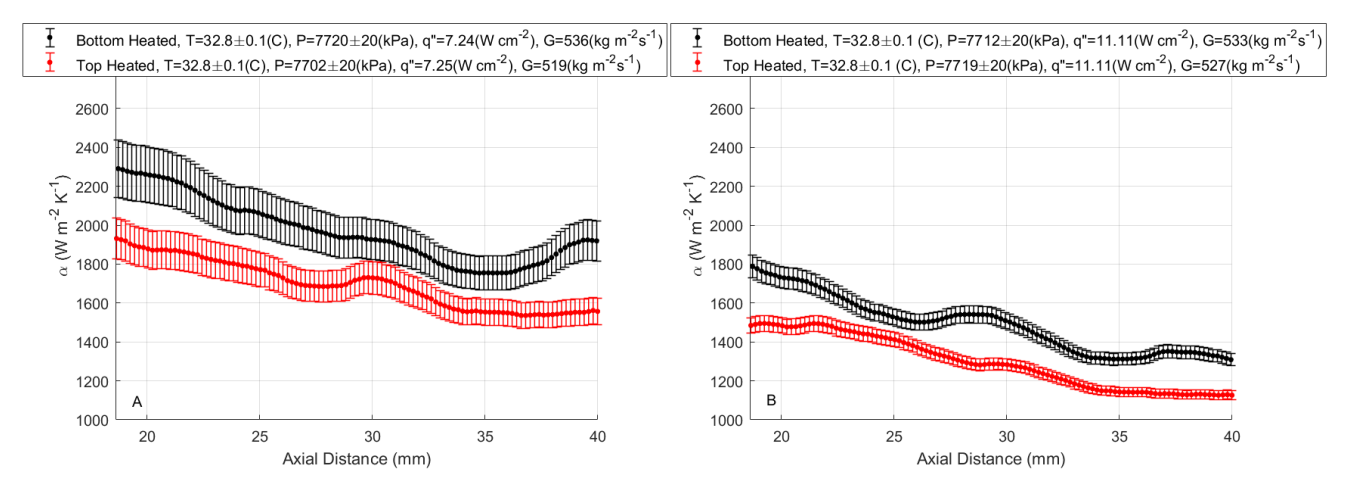


**FIGURE 5**. Developed Region of Asymmetrically Bottom and Top Heated Conditions with Constant Mass Flux ( $G = 520 \text{ kg m}^{-2} \text{ s}^{-1}$ ). A)  $q'' = 7.25 \text{ W cm}^{-2}$ , B)  $q'' = 11.1 \text{ W cm}^{-2}$ 

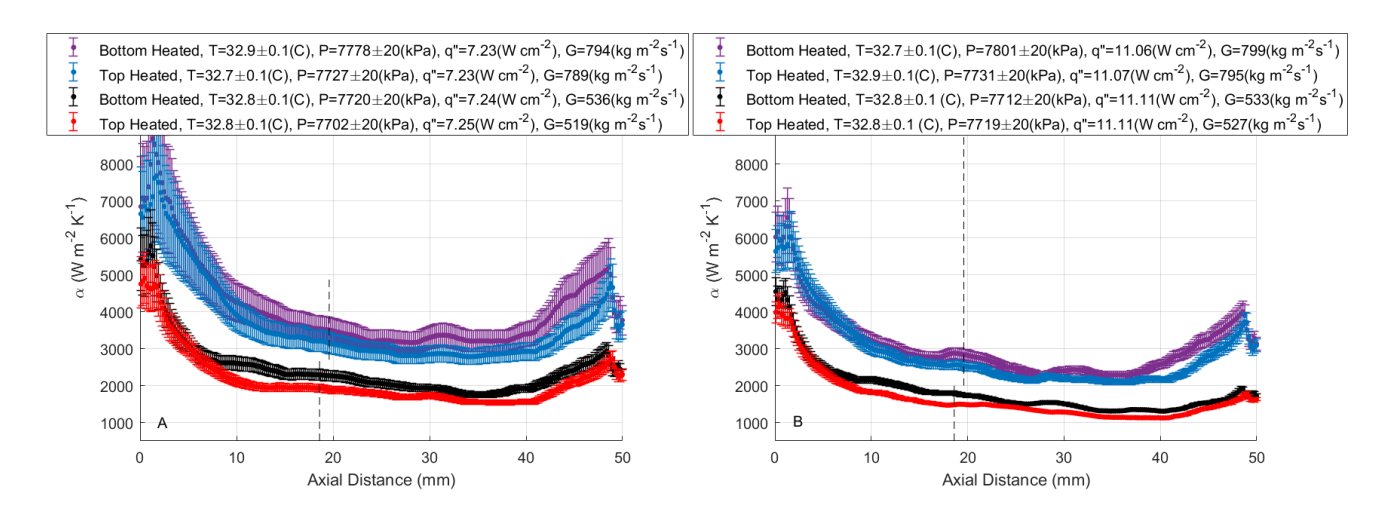


**FIGURE 6**. Asymmetrically Bottom and Top Heated Conditions with Constant Heat Flux and Both High Mass Flux ( $G = 895 \text{ kg m}^{-2} \text{ s}^{-1}$ ) and Low Mass Flux ( $G = 520 \text{ kg m}^{-2} \text{ s}^{-1}$ ). A)  $q'' = 7.25 \text{ W cm}^{-2}$ , B)  $q'' = 11.1 \text{ W cm}^{-2}$ 

line), the top and bottom heated coefficients are nearly equivalent and within experimental uncertainty. At about 5 mm into the channel, the top and bottom heated cases deviate, and the top heated coefficients drop below those of the bottom heated case and remain slightly lower, by a maximum of approximately 15 percent. Beyond an axial length of 40 mm, exit effects cause an increase in the measured heat transfer coefficient due to enhanced cooling in the outlet header, as described in Jajja [6]. Figure 5 shows a detailed view of the heat transfer coefficient in the middle of the channel, where entrance and exit effects are expected to be minimized.

There are significant differences between the low (Figure

4A) and high (Figure 4B) heat flux cases. For example, the lower heat flux has higher heat transfer coefficients and steeper gradients at both the entrance and the exit of the channel. However, there does not appear to be a significantly different effect for these conditions due to heat flux on the top heated cases compared to the bottom heated cases.

#### **Effect of Mass Flux**

Measurements were taken for both top and bottom heated conditions at mass flow rates of  $G=895~kg~m^{-2}~s^{-1}$  and  $G=520~kg~m^{-2}~s^{-1}$ . The higher mass flux cases exhibit steeper gradients near the channel's entrance and exit and have higher heat

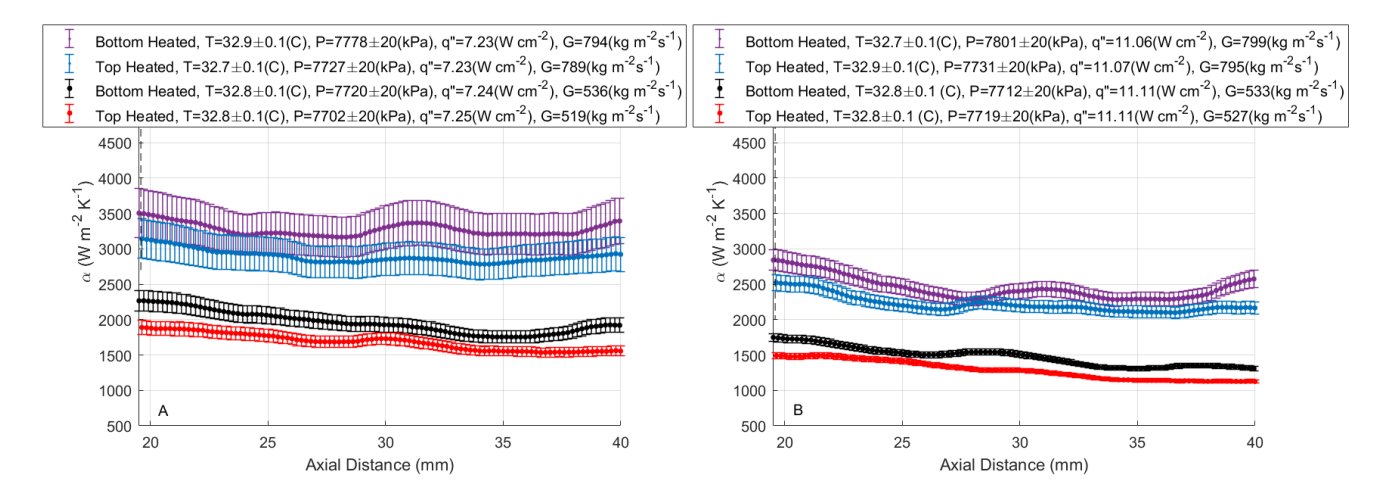


**FIGURE 7**. Developed Region of Asymmetrically Bottom and Top Heated Conditions with Constant Heat Flux and Both High Mass Flux ( $G = 895 \text{ kg m}^{-2} \text{ s}^{-1}$ ) and Low Mass Flux ( $G = 520 \text{ kg m}^{-2} \text{ s}^{-1}$ ). A)  $q'' = 7.25 \text{ W cm}^{-2}$ , B)  $q'' = 11.1 \text{ W cm}^{-2}$ 

transfer coefficients throughout the channel. Figure 7 shows a comparison of the data for the middle of the channel, where entrance and exit effects are less important. Here, the potential effects of buoyancy appear to be greater for the lower mass flux data.

For the higher mass flux, the top and bottom coefficients deviate at about 7.5 mm into the channel as opposed to the low mass flux that deviated around 5 mm. This could be due to the high mass flux cases' higher midstream velocities suppressing the turbulent heat transfer away from the wall. The exit region for the high mass flux has a slightly larger difference between the top and bottom heated cases than that of the lower mass fluxes.

#### CONCLUSION

In this work, we used IR thermography to measure local heat transfer coefficients of near-critical carbon dioxide in a horizontal microchannel duct heated from a single wall. Top and bottom heating orientation were considered. Based on the screening criteria of McEligot et al. [10], flow acceleration effects were not expected to be important, while the Petukhov and Polykov [11] criteria suggested buoyancy was strong enough to alter thermal transport for all data.

The results show a degradation of heat transfer for topheated cases. For the lower mass flux cases, this degradation was between 13 and 15 percent, whereas for the higher mass flux it was between 10 and 12 percent.

These initial data suggest that buoyancy should be considered when developing correlations and models for predicting near-critical heat transfer in non-uniformly heated ducts. Further research is required on (1) developing appropriate buoyancy criteria for non-uniformly heated, rectangular channels, (2) un-

derstanding coupled effects of flow acceleration and buoyancy, and (3) developing a mechanistic based model of near-critical thermal transport that captures the effects of flow acceleration, buoyancy, and thermophysical property variation.

#### **ACKNOWLEDGMENT**

We acknowledge the help and training provided by Saad Jajja on the safe and accurate operation of the experimental setup, and for consultation on data analysis methodology. Funding for this work was provided by NSF Grant 1604433.

#### **REFERENCES**

- [1] Fronk, B. M., and Rattner, A. S., 2016. "High-Flux Thermal Management with Supercritical Fluids". *Journal of Heat Transfer,* 138(12), 12.
- [2] Pioro, I. L., and Duffy, R. B., 2007. Heat Transfer and Hydraulic Resistance at Supercritical Pressures in Power-Engineering Applications. ASME.
- [3] Pioro, I. L., Khartabil, H. F., and Duffey, R. B., 2004. "Heat transfer to supercritical fluids flowing in channels Empirical correlations (survey)". In Nuclear Engineering and Design, Vol. 230, North-Holland, pp. 69–91.
- [4] Jajja, S. A., Zada, K. R., and Fronk, B. M., 2019. "Experimental investigation of supercritical carbon dioxide in horizontal microchannels with non-uniform heat flux boundary conditions". *International Journal of Heat and Mass Transfer*, 130, 3, pp. 304–319.
- [5] Jajja, S. A., Sequeira, J. M., and Fronk, B. M., 2020. "Geometry and orientation effects in non-uniformly heated

- microchannel heat exchangers using supercritical carbon dioxide". Experimental Thermal and Fluid Science, 112.
- [6] Jajja, S. A., 2020. "Turbulent Heat Transfer of Supercritical Carbon Dioxide in the Proximity of the Pseudo-Critical Point with Non-Uniform Heat Flux Boundary Conditions". PhD thesis, Oregon State University.
- [7] Miropol'ski, Z., and Shitsman, M., 1958. "About calculation methods of heat transfer to water and steam at near-critical region". *Soviet Energy Technology*, *1:8*(11).
- [8] Ornatsky, A., Glushchenko, L., and Siomin, E., 1970. "The research of temperature conditions of small diameter parallel tubes cooled by water under super- critical pressures.". In Proceedings of the Fourth International Heat Transfer Conference.
- [9] Jackson, J. D., and Hall, W. B., 1979. "Forced Convection Heat Transfer to Fluids at Supercritical Pressure". *Turbulent Forced Convection in Channels and Bundles*.
- [10] McEligot, D. M., Coon, C. W., and Perkins, H. C., 1970. "Relaminarization in tubes". *International Journal of Heat and Mass Transfer,* 13(2), 2, pp. 431–433.
- [11] Petukhov, B. S., and Polyakov, A. F., 1988. *Heat Trans*fer in Turbulent Mixed Convection. Hemisphere Publishing Corporation.
- [12] Figliola, R. S., and Beasley, D. E., 2010. *Theory and Design for Mechanical Measurements*, 5 ed. John Wiley and Sons.
- [13] Mceligot, D. M., and Jackson, J. D., 2004. "Deterioration" criteria for convective heat transfer in gas flow through non-circular ducts". *Nuclear Engineering and Design*, **232**, pp. 327–333.
- [14] Osborne, D. G., and Incropera, F. P., 1985. "Experimental study of mixed convection heat transfer for transitional and turbulent flow between horizontal, parallel plates". *International Journal of Heat and Mass Transfer*, **28**(7), 7, pp. 1337–1344.